The Fifth International Symposium – Supercritical CO_2 Power Cycles
March 29–31, 2016, San Antonio, Texas

DEPENDENCE OF THERMAL EFFICIENCY ON RECEIVER TEMPERATURE OF SOLAR THERMAL POWER SYSTEMS COMBINED WITH SUPERCRITICAL CO2 GAS TURBINE CYCLE AND BRAYTON CO2 GAS TURBINE CYCLE

Yasushi Muto
Research Associate
Tokyo Institute of Technology
O-okayama, Meguro-ku, Tokyo, Japan
muto@nr.titech.ac.jp

Noriyuki Watanabe
Research Associate
Tokyo Institute of Technology
O-okayama, Meguro-ku, Tokyo, Japan
watanabe.n.ac@m.titech.ac.jp

Masanori Aritomi
Research Associate
Tokyo Institute of Technology
O-okayama, Meguro-ku, Tokyo, Japan
aritomimasa@yahoo.co.jp

Takao Ishizuka
Research Associate
Tokyo Institute of Technology
O-okayama, Meguro-ku, Tokyo, Japan
takao.i@nr.titech.ac.jp


Master of Nuclear Engineering of Tokyo University. Former employee of the Japan Atomic Energy Research Institute. Research on gas turbines.


Dr. of Heat Transfer of Tokyo Institute of Technology. Research on condensation heat transfer enhancement.


Dr. of Heat Transfer of Tokyo Institute of Technology. Prof. of Research Laboratory for Nuclear Engineering, Tokyo Institute of Technology, Emeritus Professor.


Dr. of Heat Transfer of Tokyo Institute of Technology. Former employee of Toshiba Corp. Research on heat transfer of two-phase flow.

ABSTRACT

A supercritical CO_2 gas turbine cycle can achieve extremely high cycle thermal efficiency using compression work reduction near the critical point. However, the cycle must be provided with a bypass circuit, which presents some difficulty for the compressor design and operation. In addition, very high pressure of 20 MPa is not easily accommodated in the plant design. A Brayton CO_2 GT cycle is more readily used in a design, but its achievable cycle thermal efficiency is 4% less than that for the supercritical CO_2 GT cycle. The cycle thermal efficiency values are still higher than those for other gas turbine cycles, e.g. He and N_2 gas. Solar power generation systems, which consist of a tower top receiver cooled by Na, and with a Na-Al-CO_2 heat exchanger provided with the above two CO_2 GT-cycles have been examined. The values of the receiver efficiency are dependent not only on the Na outlet temperature but on the inlet temperature. The parametric design calculations of the Na-Al-CO_2 heat exchanger have been conducted. A thermal energy allocated to the heat storage is assumed 30%. The values of the

CO_2 inlet and outlet temperatures for the supercritical CO_2 cycle and the Brayton CO_2 cycle are fixed to achieve the respective maximum cycle thermal efficiencies. Values of spacing between the Na tubes and the CO_2 tubes are adjusted to achieve the required heat transfer loads. The lower receiver inlet Na temperature becomes possible for the Brayton CO_2 cycle than for the supercritical CO_2 cycle due to the higher heat transfer capacity. However, the lower receiver inlet Na temperature results in the smaller melting Al area and the smaller heat storage capacity. The design receiver Na inlet temperatures are 600°C, 610°C and 640°C for the supercritical CO_2 cycle with 60.5mm tube, for the supercritical CO_2 cycle with 48.6mm tube and the Brayton CO_2 cycle, respectively. In this condition, the values of the total thermal efficiency are 22.6%, 22.5% and 20.0% for the supercritical CO_2 cycle with 60.5mm tube, for the supercritical CO_2 cycle with 48.6mm tube and the Brayton CO_2 cycle, respectively. However, it is difficult to decide which cycle is superior. More comprehensive design studies including the capital cost and the operation cost are needed for the final decision.

INTRODUCTION

The supercritical CO_2 gas turbine cycle can achieve high cycle thermal efficiency because of the small compression work near the critical point (31.06°C, 7.38 MPa) and also because of the effective use of thermal energy using a recuperator (Kato, 2004; Muto, 2013). The recuperator raises the temperature of compressor outlet gas flowing to the heat source. Therefore, the heat source temperature should be sufficiently high not only at the outlet but also at the inlet. Few heat sources with such characteristic are available. Only nuclear energy and solar energy meet the requests. An earlier paper examined application of a supercritical CO_2 cycle to solar power generation (Muto, 2015). A beam-down type solar energy concentration system was used in that study, where the sun beams are collected in the cavity provided at the top of the receiver. Once the sunlight reaches within the cavity, most is retained within the cavity because the open space is limited. At the high temperatures, radiation energy is emitted, which is proportional to the fourth order of the absolute temperature. Then, the receiver efficiency becomes higher than the tower top receiver, even at high temperatures. Commercially available solar thermal power plants use a molten salt (a mixture of KNO_3 and $NaNO_3$). However, this molten salt can only be used below 600°C. In this case, the turbine inlet temperature must be lower than 550°C. This temperature level is not sufficiently high to use the gas turbine cycle effectively. Therefore, aluminum was used as the heat transfer and heat storage material. The thermal conductivity of metal aluminum is extremely high. Its specific heat is large. Therefore, it is a good heat transfer material. Additionally, its melting temperature is 660°C. The latent heat is 397 kJ/kg, which is extremely large. Therefore, the aluminum is an excellent heat storage material. The previous system consisted of the beam down solar beam collection receiver, an aluminum blanket and the supercritical CO_2 gas turbine. Although the beam-down system can minimize heat loss from the receiver, the receiver must be placed at a high position such as 30 m. The large amount of aluminum is extremely heavy and cannot be provided at such high place. Therefore, the system should be modified.

Supercritical gas turbine cycles of two types are considered. The first is the usual supercritical CO_2 cycle scheme, which incorporates two recuperators and a bypass compressor circuit as presented in Fig. 1. The pressure is higher than 20 MPa. Very high cycle thermal efficiency can be achieved with this system. However, parallel compression circuits and very high pressure cause great difficulties. The other is a traditional Brayton cycle presented in Fig. 2. In this system, the achievable cycle thermal efficiency is lower than the first because effective recuperation cannot be achieved as a result of the thermal capacity difference between the high-temperature side and the low-temperature side. However, no difficult design problem exists.

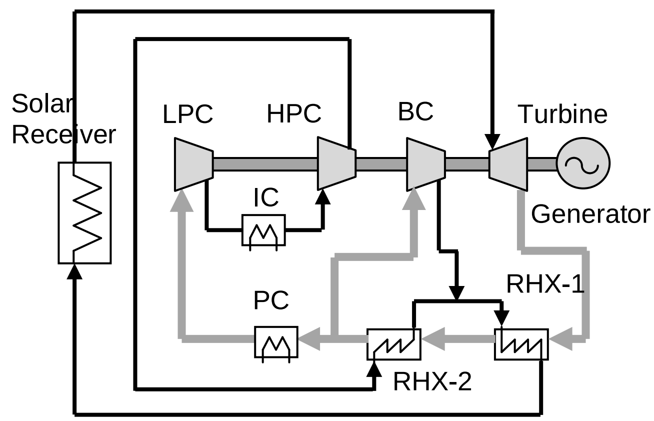

Fig. 1. Supercritical CO_2 gas turbine cycle.

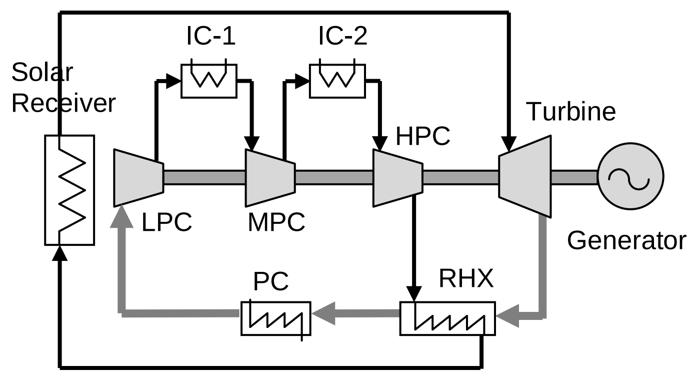

Fig. 2. Brayton CO_2 gas turbine cycle.

In an earlier study, the two systems were compared for the application of 100 MW solar power. The cycle thermal efficiency of the Brayton cycle CO_2 gas turbine is 4% less than that of the supercritical CO_2 gas turbine, but it is 3% higher than that of the ideal (He) cycle gas turbine at the turbine inlet temperature of 650°C. Regarding the component design, for the supercritical scheme, the compressor design is much more difficult and the recuperator size becomes much larger than for the Brayton cycle scheme.

In this paper, the achievable cycle thermal efficiency values that are dependent on the heat source inlet temperature are calculated and compared for these two cycle schemes under the new prerequisites. The previous system was improved, i.e., a new system depicted in Fig. 3 consists of a tower top receiver cooled by liquid Na. The liquid Na is a fluid with good heat transfer and heat transport properties. To store the thermal energy, the aluminum blanket was replaced by a Na-Al-CO_2 heat exchanger. The heat loss from the surface of receiver is strongly dependent on both the surface temperature and the surface area size. They are related strongly to the Na inlet and outlet temperatures. Even at the same outlet temperature, the higher inlet temperature results in greater heat loss. The lower Na temperature requires lower CO_2 inlet temperature, which strongly reduces the cycle thermal efficiency. In addition, the high pressure CO_2 requires a thick wall for the heat transfer tubes. Because the thermal conductivity of the stainless steel, including Alloy 800H is not good, it has higher heat resistance, which degrades the heat transfer performance. First, the receiver efficiency dependence of the Na temperature is calculated. Then, the aluminum heat exchanger design calculation is conducted and the CO_2 inlet temperature dependence on the Na temperature is calculated. Finally, the cycle thermal efficiency of CO_2 cycles and the total thermal efficiency are revealed.

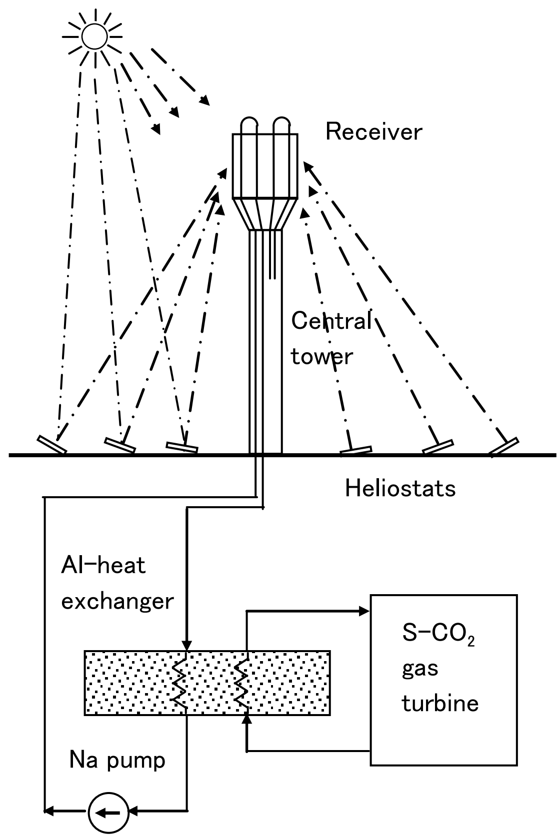

Fig. 3. Solar thermal power generation system with Na cooled receiver, Al heat exchanger and CO_2 gas turbine.

SODIUM COOLED SOLAR RECEIVER PERFORMANCE

Concentrating central tower top receivers have been used. The structure is assumed to be a cylinder provided with an annular flow channel. The solar energy capacity was assumed to be 125 MW based on a reference design (Hasuike, 2006). In this case, the solar field is a ring with the 800 m outer diameter and 52.6 m inner diameter, with 103 m height of the upper focus. The receiver was newly designed. The shell material of the solar collecting surface is alloy800H, which is a generally used and inexpensive high-temperature material. The outlet temperature of Na is 700°C. In this system, the phase change of aluminum is used for heat storage to generate the necessary power at night. A minimum temperature difference of 40°C is regarded as needed for heat transfer between the Na and the aluminum melting point of 660°C. At higher temperatures, the energy loss increases sharply. Therefore, 700°C was selected. The shell design temperature was chosen as 800°C. In this case, the allowable stress of alloy800H is 15 MPa. The maximum allowable shell temperature is 780°C for the design margin of 20°C. The inlet pressure of Na was assumed to be 0.13 MPa to afford 0.03 MPa pressure drop in the Na circuit. Based on these assumptions, the outer shell diameter, the shell wall thickness, and the

Na flow channel width were determined to achieve the maximum solar energy received. The receiver specifications are presented in Table 1.

Table 1 Design specifications of the receiver cooled by Na

Na inlet temperature °C	Shell outer diameter m	Shell wall thickness mm	Na flow channel width mm	Na flow rate kg/s	Receiver efficiency %
400	9	11.0	10	239.2	72.928
420	9	11.0	10	254.6	72.437
440	9.1	11.0	10	271.4	71.695
460	9.1	11.0	10	291.8	71.160
480	9.1	11.0	10	315.8	70.606
500	9.1	11.0	10	344.6	70.036
520	9.1	11.0	10	379.7	69.447
540	9.1	11.0	11	423.1	68.793
560	9.2	11.2	12	476.0	67.719
580	9.3	11.4	13	546.3	66.605
600	9.4	11.4	14	645.3	65.565
620	9.4	11.4	16	797.0	64.785
640	9.5	11.6	20	1041.3	63.482
660	9.7	11.8	36	1513.6	61.515

In the table, the receiver efficiency is defined as the thermal energy transferred to Na over the thermal energy collected on the shell surface (125 MW). As the energy loss, the radiation loss and convection loss were considered.

The Na flow rate and the receiver efficiency are depicted in Fig. 4. As the figure shows, the effects of the value of the Na inlet temperature on the receiver efficiency are known to be large, i.e., 10% difference exists between 400°C and 660°C in the Na inlet temperature. A significant amount of temperature difference between the Na inlet temperature and the CO_2 inlet temperature is unavoidable as described in the following section. The CO_2 inlet temperature must be high enough to use the recuperator effectively. Therefore, the higher temperature regime becomes important.

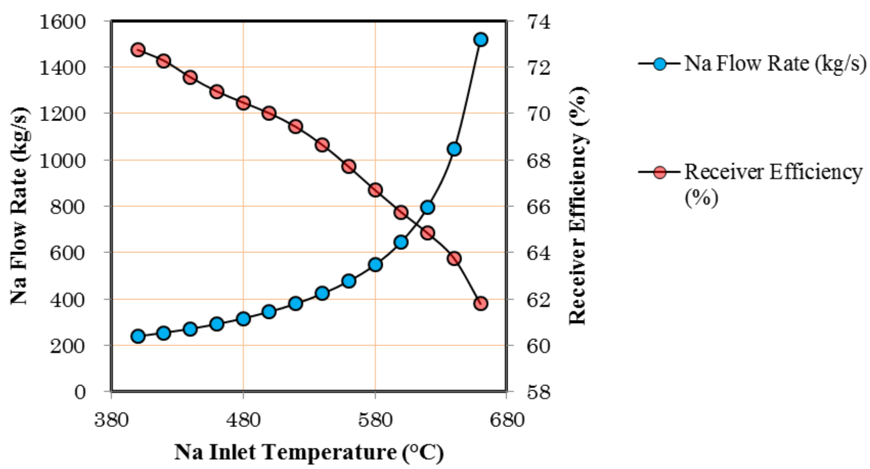

Fig. 4. Na flow rate and the receiver efficiency dependence on the Na inlet temperature.

Na-Al-CO_2 HEAT EXCHANGER PERFORMANCE

The sodium leaving the receiver is transported to the Na-Al-CO_2 heat exchanger at the same temperature because the heat loss in the piping is assumed to be neglected. The U-shaped sodium heat transfer tubes penetrate an aluminum block placed horizontally in a box casing. The U-shaped CO_2 heat transfer tubes also penetrate the aluminum block horizontally in parallel with Na tubes. The thermal energy is transferred from the Na to the aluminum. Then it is transmitted by heat conduction via the aluminum and is then transferred to CO_2. Both the sodium tubes and the CO_2 tubes are alternately arranged each by each closely to achieve good heat transfer performance. The box casing including the aluminum block is installed in a leak-tight vessel. Gaps filled by argon gas are provided between the casing and the vessel at the sides and top. The space of the gap allows thermal expansion of both the U tubes and also of the aluminum block. In this report, the daytime is assumed 12 hours from 6 a.m. to 8 p.m. and the full sunshine energy can be collected. Regarding the demand, 12 hours of the daytime is 100% and at night, 100% from 6 p.m. to 8 p.m. and 60% from 8 p.m. to the midnight and 10% from the midnight to 6 a.m., the total night demand becomes 5 hours. Then, 12/17=70% and 5/17=30% are needed in the daytime and at night, respectively. Therefore, the heat storage ratio is 30%. The total sunbeam energy is 125 MW and the expected receiver efficiency will be around 65%. The total thermal energy becomes 3,510,000 MJ for 12 hours. The storage energy requirement becomes 1,053,000 MJ. From this data an aluminum inventory and then the vessel dimensions are determined. The vessel is rectangular: 8.6 m wide, 2.5 m high, and 60 m long. In all, 3,000 tons of aluminum is installed. If 30% of aluminum is used effectively for the phase change, then the latent heat capacity of aluminum becomes 357,000 MJ because the latent heat of aluminum is 397 kJ/kg. After cooling to less than 660°C, the thermal energy attributable to the sensible specific heat of aluminum (0.90 kJ/kg/K) is used. If a temperature change of 250°C is available, the sensible heat capacity becomes 675,000 MJ, which is equivalent or larger than the latent heat. The total heat capacity is 1032,000 MJ, which agree with the above heat storage requirement. The tube material is Alloy800H. The diameters of both the Na and CO_2 tubes are 60.5 mm. The smaller Na and CO_2 tube diameters of 48.6 mm were also examined for comparison. The wall thicknesses of CO_2 tubes are dependent on the CO_2 pressure. The design pressures are, respectively, 24 MPa for the 20 MPa supercritical CO_2 tubes and 9.6 MPa for the 8 MPa Brayton CO_2 tubes. The design temperature is 680°C, which is the aluminum melting temperature of 660°C plus a control margin of 20°C. At this temperature, the allowable stress of Alloy 800H is 39.85 MPa. Under these assumptions, the minimum wall thickness was determined respectively to 12.9 mm for the supercritical CO_2 tube and 6.3 mm for the Brayton CO_2 tube. This larger wall thickness for the supercritical CO_2 results in the large heat resistance and considerable detrimental effect on the temperature distribution, as described later.

The following are basic heat transfer equations for the heat exchanger.

$$\eta_R Q_{Sun} = \dot{m}_{Na} Cp_{,Na}\left(T_{Na,Out} - T_{Na,in}\right) \tag{1}$$

Where

$$\eta_R = \text{Function}\left(T_{Na,Out}, T_{Na,in}, \dot{m}_{Na}\right)$$

$$(1-\beta)\eta_R Q_{Sun} = \dot{m}_{CO2} Cp_{,CO2}\left(T_{CO2,Out} - T_{CO2,In}\right) \tag{2}$$

$$(1-\beta)\eta_R Q_{Sun} = K_H \times S \times \Delta T_m \tag{3}$$

Where

$$K_H = \text{Function}\left(T_{Na,In}, T_{Na,Out}, \dot{m}_{Na}, T_{CO2,In}, T_{CO2,Out}, \dot{m}_{CO2}, S_{tube}\right)$$

$$\triangle T_m = Function(T_{Na,Out}, T_{Na,in}, T_{CO2,Out}, T_{CO2,In})$$

In those equations, the following variables are used.
Q_{Sun} = Total sun beam energy collected by the receiver
η_R = Receiver efficiency, which is the thermal energy transmitted to the sodium over the thermal energy collected by the receiver
β = Ratio of the thermal energy stored in the aluminum over the thermal energy transmitted from the sodium
$\dot{m}_{Na}$ = Sodium mass flow rate
$\dot{m}_{CO2}$ = CO_2 mass flow rate
$T_{Na,Out}$ = Receiver outlet Na temperature = heat exchanger inlet Na temperature
$T_{Na,In}$ = Receiver inlet Na temperature = heat exchanger outlet Na temperature
$T_{CO2,In}$ = CO_2 heat exchanger inlet temperature
$T_{CO2,Out}$ = CO_2 heat exchanger outlet temperature
$Cp_{,Na}$ = Specific heat of sodium
$Cp_{,CO2}$ = Specific heat of CO_2
K_H = Overall heat transfer coefficient
S_{tube} = Horizontal tube spacing between Na tube and CO_2 tube
S = Total heat transfer area
$\triangle T_m$ = Logarithmic temperature difference

In fact, equation (1) is also valid for the receiver and is already solved by the parametric values of $T_{Na,In}$. Here, $T_{Na,Out}$ is assumed to be 700°C. The values of $\eta_R Q_{Sun}$ and m_{dotNa} are obtained for the parametric values of $T_{Na,In}$. In the heat exchanger, except for $T_{Na,In}$, m_{dotNa}, Four variables exist: $T_{CO2,In}$, $T_{CO2,Out}$, $m_{dot,CO2}$ and K_H. As results of a preliminary survey, it was revealed that the values of $T_{CO2,In}$ and $T_{CO2,Out}$ should be selected so as to achieve the maximum cycle thermal efficiency. Specifically, the values of $T_{CO2,In}$ and $T_{CO2,Out}$ are 466.71°C and 650°C for the supercritical CO_2 cycle and 396.75°C and 650°C for the Brayton CO_2 cycle, respectively. Therefore the values of the cycle thermal efficiency are fixed, which are 49.19% and 44.83% for the supercritical CO_2 cycle and the Brayton CO_2 cycle, respectively. The value of $m_{dot,CO2}$ are obtained from the values of $(1-\beta)\eta_R Q_{Sun}$. After all, the equations are solved for the two variables: $T_{Na,In}$ and K_H. Though the overall heat transfer coefficient K_H consists of many variables, only the value of horizontal tube spacing between Na tubes and CO_2 tubes are varied and adjusted to satisfy the equations.
The calculated values of thermal efficiency are shown in Fig. 5. Here, the value of the thermal efficiency is simply given by the following equation.

$$\text{Thermal efficiency} = (Receiver\ efficiency) \times (1-\beta) \times (Cycle\ thermal\ efficiency)$$

Since the CO_2 temperatures are fixed, the values of cycle thermal efficiency are constant, which are 49.19% and 44.83% for the supercritical CO_2 cycle and the Brayton CO_2 cycle, respectively. The temperature dependence of the thermal efficiency is simply due to that of the receiver inlet Na temperature.

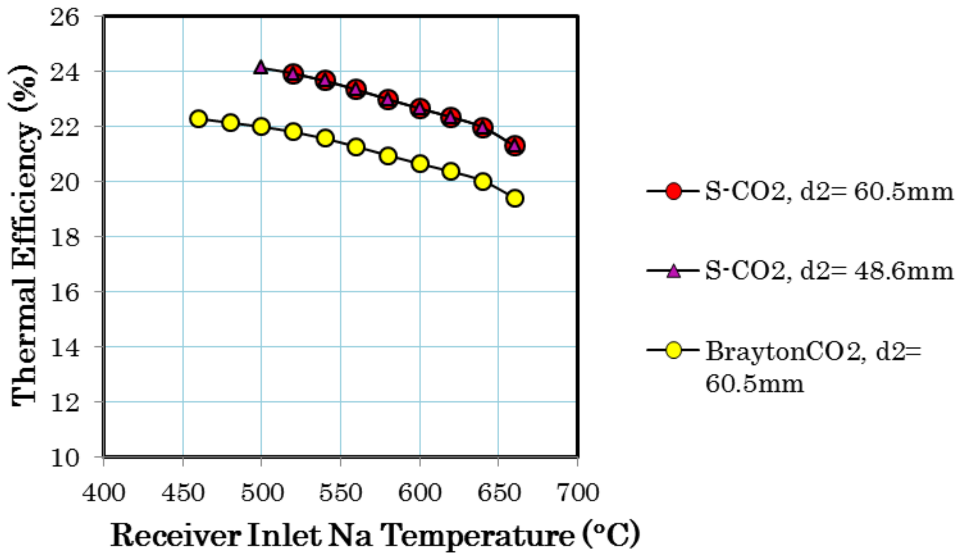

Fig. 5. Thermal efficiency dependence on the receiver inlet Na temperature.

As the thermal efficiency increases, the heat load on the Na-Al-CO_2 heat exchanger increases. To increase the required heat load, the space between Na tubes and CO_2 tubes should become smaller. Under the assumption that the minimum space is twice of the tube outer diameter, the lowest allowable receiver inlet temperature becomes 520°C, 500°C and 460°C, for the supercritical CO_2 cycle with the tube diameter of 60.5mm, the supercritical CO_2 cycle with the tube diameter of 48.6mm and the Brayton CO_2 cycle, respectively. Therefore, the lower receiver inlet temperature can be used for the Brayton CO_2 cycle than the supercritical CO_2 cycle. However, the lower Na inlet temperature results in the reduction of melted Al area and then, the reduction of the available amount of the latent heat. The percentage values of the melted Al area are shown in Fig. 6.

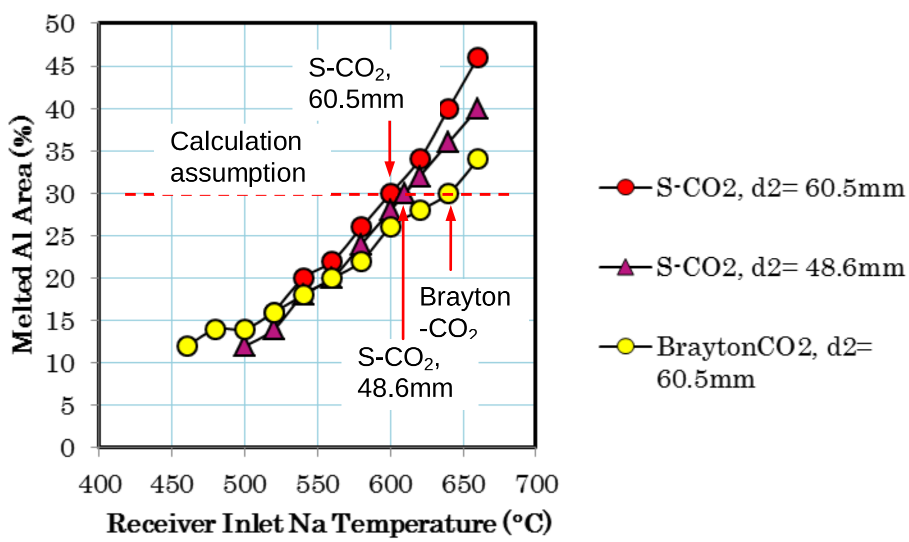

Fig. 6. Melted Al area dependence on the receiver inlet Na temperature.

In the calculations, the solar thermal energy used for the heat storage and then, the melted Al area is roughly assumed 30%, though not the latent heat but also the sensible heat is used for the heat storage. From this figure, the values of the receiver inlet Na temperature corresponding to the melted Al area of 30% for the supercritical CO_2 cycle with 60.5mm tube, the supercritical CO_2 cycle with 48.6mm tube and the Brayton CO_2 cycle are known to be 600°C, 610°C and 640°C, respectively. These are selected as the conclusive results. In these conditions, the respective values of the cycle thermal efficiency are 22.63%, 22.48% and 20.00%. For these conditions, Table 2 shows the system performance.

Table 2 Design calculation results for the selected points

Design parameters		S-CO_2 cycle with D60.5mm	S-CO_2 cycle with D48.6mm	Brayton CO_2 cycle
Receiver inlet Na temperature	°C	600	610	640
Receiver outlet Na temperature	°C	700	700	700
Na flow rate	kg/s	646.98	713.91	1045.69
Receiver efficiency	%	65.73	65.28	63.75
HX CO_2 inlet temperature	°C	466.71	466.71	396.75
HX CO_2 outlet temperature	°C	650	650	650
CO_2 flow rate	kg/s	252.19	250.45	183.89
Cycle thermal efficiency	%	49.19	49.19	44.83
Na and CO_2 tubes spacing	mm	209	254	326
Number of vertical tube-lines	-	8	10	8
Number of horizontal tube-rows	-	144×2	118×2	92×2
Melted Al area	%	30	30	30
Thermal efficiency	%	22.63	22.48	20.01

Though the thermal efficiency is 2 or 3% higher for the supercritical CO_2 cycle than for the Brayton CO_2 cycle, it should be pointed out that more numbers of tubes are needed for the former than the latter due to the lower overall heat transfer coefficient. Therefore, the capital cost should be estimated and compared.

The temperature distributions are depicted in Fig. 7 for the 20 MPa CO_2 with 60.5mm tube and in Fig. 8 for the 20 MPa CO_2 with 48.6mm tube and in Fig. 9 for the 8 MPa CO_2, respectively, for the above cases. The Al temperatures are shown to exceed 660°C in the 30% area. From these figures, relative values of the thermal resistances can be estimated. The values of wall temperature difference are larger than other temperature differences in the 20 MPa of the supercritical CO_2 GT cycle. This is because of the higher thermal resistance in the 20 MPa CO_2 thick tube wall. Though the thermal wall resistance is slightly improved for the smaller 48.6mm tube, the improvement from the 60.5mm tube is small. As for the Brayton CO_2 cycle, the values of temperature difference are known to be similar.

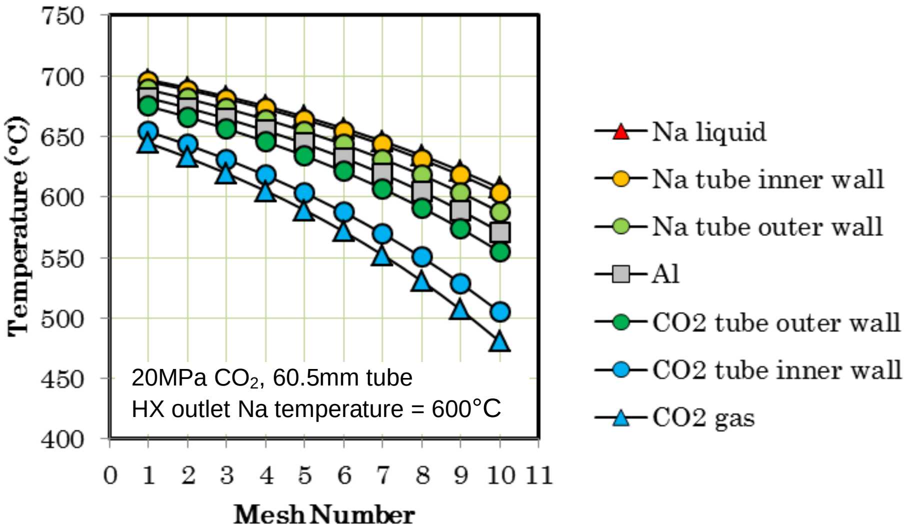

Fig. 7. Temperature distribution in the Na-Al-CO_2 heat exchanger for the 20 MPa CO_2 with 60.5mm tube**.**

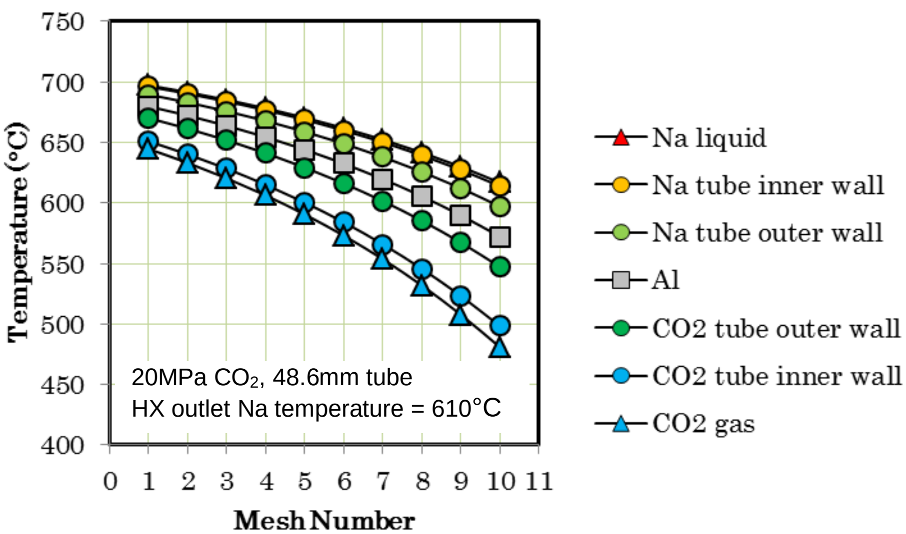

Fig. 8. Temperature distribution in the Na-Al-CO_2 heat exchanger for the 20 MPa CO_2 with 48.6mm tube**.**

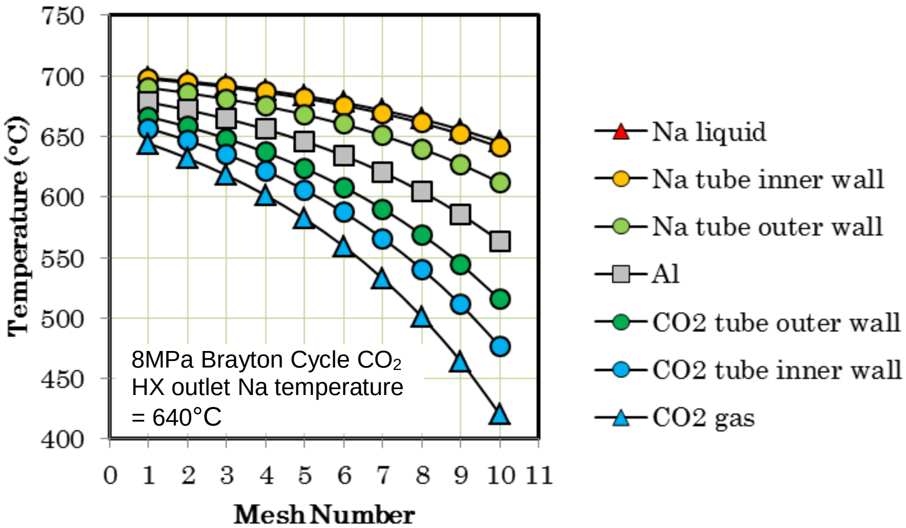

Fig. 9. Temperature distribution in the Na-Al-CO_2 heat exchanger for the 8 MPa CO_2.

CYCLE THERMAL EFFICIENCY OF SUPERCRITICAL CO_2 GAS TURBINE CYCLE

Two flow schemes are considered. One is the supercritical CO_2 cycle with a bypass circuit as presented in Fig. 1. The other is the Brayton CO_2 cycle, as presented in Fig. 2.

As the number of intercoolers increases, the cycle thermal efficiency increases. However, the benefit becomes saturated as the number of intercoolers increases. In addition, too many intercoolers make the system complicated. In the case of the supercritical CO_2, two compressors are necessary. Then, only one intercooler was used. Regarding the Brayton CO_2 cycle, two intercoolers, and three compressors were used. The three numbers of compressors are connected in series. Therefore, no operational problem is expected for this scheme. The addition of more than two intercoolers can increase the cycle thermal efficiency slightly. The amount of increase is so limited that the advantage is cancelled by the detrimental effects of the complex system. Therefore, two intercoolers were used.

The values of cycle thermal efficiency are calculated. The gas properties of CO_2 such as enthalpy and entropy are based on a computer dataset: “PROPATH” (PROPATH Group, 1990).

The values of adiabatic efficiency are determined based on the conceptual design (Muto, 2010) of the gas turbine of the 1,500 MWe commercial power plants for the Na-cooled fast reactor.

The value of recuperator effectiveness gives a great effect on the values of the cycle thermal efficiency. Generally speaking, the following definitions of recuperator effectiveness are used.

$$\eta_{RHX,Hot} = \frac{T_{H,in} - T_{H,out}}{T_{H,in} - T_{C,in}}$$

$$\eta_{RHX,Cold} = \frac{T_{C,out} - T_{C,in}}{T_{H,in} - T_{C,in}},$$

In those equations, the following variables are used.

$\eta_{RHX,Hot} =$ High-temperature side temperature effectiveness

$\eta_{RHX,Cold} =$ Low-temperature side temperature effectiveness

$T_{H,in}$ = High-temperature side inlet temperature

$T_{H,out}$ = High-temperature side outlet temperature

$T_{C,in}$ = Low-temperature side inlet temperature

$T_{C,out}$ = Low-temperature side outlet temperature

For a typical gas turbine cycle such as a helium turbine, the values of the high-temperature side and low-temperature side are almost equal. For S-CO_2, however, these values differ considerably. Therefore, for these analyses, the next average value $\eta_{RHX,av}$ of the high-temperature and low-temperature side is adopted for the calculation base.

$$\eta_{RHX,av} = \frac{1}{2}\left(\eta_{RHX,Hot} + \eta_{RHX,Cold}\right)$$

Based on our previous experience, the value of 91% is assumed as the value at which a recuperator design of reasonable size is possible.

Assumptions for the two cycles are shown in Table 3.

Table 3 Assumptions for the cycle calculations.

Items		Supercritical CO_2 cycle	Brayton CO_2 cycle
Turbine inlet temperature	°C	650	650
Compressor inlet temperature	°C	35	35
Turbine adiabatic efficiency	%	92	92
Compressor adiabatic efficiency	%/ machine	88	88
Pressure loss (ratios over the inlet pressure)			
Na-Al-CO_2 heat exchanger	%	1.0	1.0
Recuperator high-temperature side	%/ unit	1.2	1.2
Recuperator low-temperature side	%/ unit	0.4	0.4
Precooler	%	1.0	1.0
Intercooler	%/ unit	0.8	0.8
Recuperator average temperature effectiveness	%/ unit	91	91

The values of cycle thermal efficiency are shown in Fig. 10. The cycle thermal efficiency increases with the pressure increase. The pressure increase rate has an inclination to saturate with the pressure increase. As for the Brayton cycle, though the value of the cycle thermal efficiency increases linearly with the pressure, there exists the maximum possible pressure as shown in Fig. 11.

The values of the CO_2 inlet temperature of the Na-Al-CO_2 heat exchanger are 466.71°C and 396.75°C for the supercritical CO_2 cycle and the Brayton CO_2 cycle, respectively. The lower temperature is desirable from the aspect of the logarithmic mean temperature difference in one hand, but it becomes drawback in the aspect of the Al melting area on the other hand. To clarify these effects, more detailed calculations are needed.

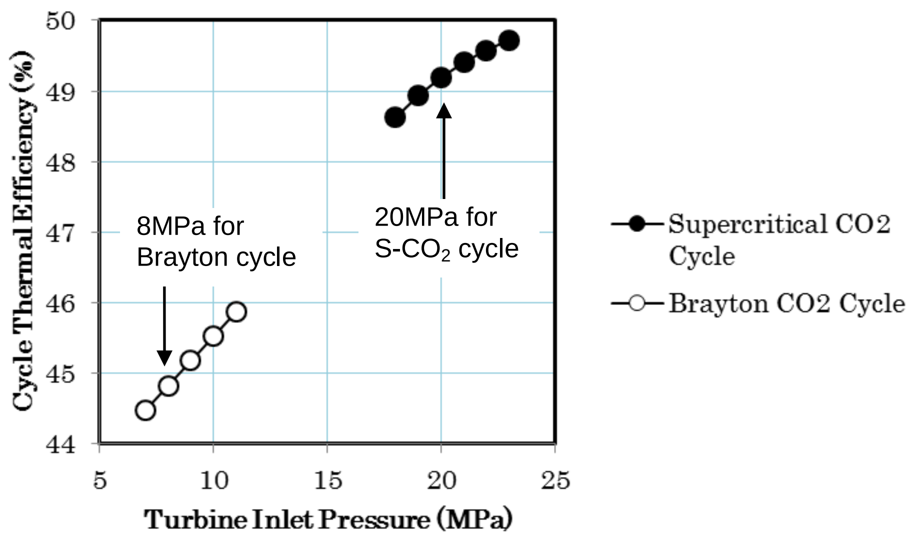

Fig. 10. Pressure dependence of the cycle thermal efficiency for the supercritical CO2 cycles.

Figure 11 shows the minimum end temperature difference of the recuperator. In case of the Brayton CO_2 cycle, the value of the minimum end temperature difference decreases markedly with the pressure increase. 9MPa or 10MPa of the pressure will be possible. However, a sufficient margin is desirable for the operation of the lower turbine inlet temperature. Therefore, 8 MPa was selected. As for the supercritical CO_2 cycle, 22 MPa of pressure may be appropriate though the 20 MPa was selected.

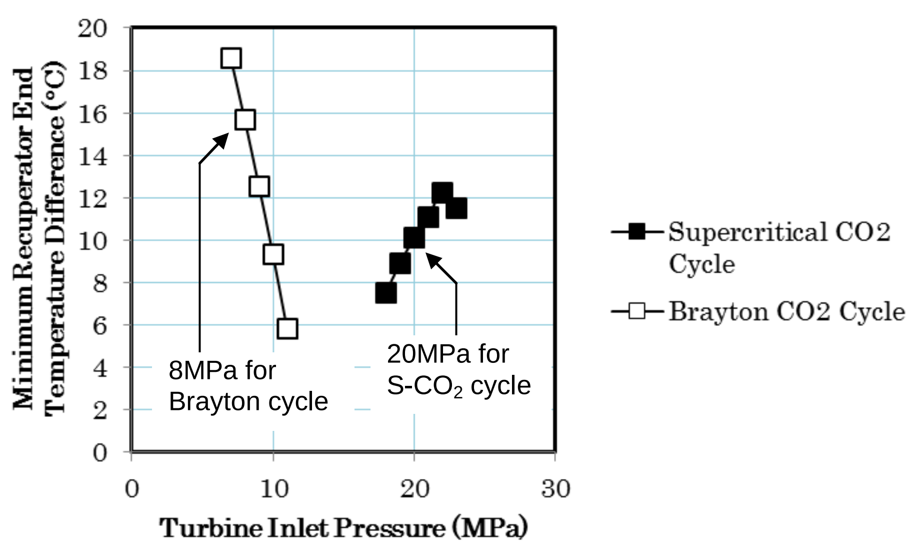

Fig. 11. Pressure dependence of the minimum recuperator end temperature difference for the supercritical CO_2 cycles.

TOTAL SYSTEM PERFORMANCE

The values of the thermal efficiency are shown in Table 2. The values of the thermal efficiency of 20 – 22% seem moderate, however, the definitions must be considered carefully. First, the value corresponds to the daytime power generation while 30% energy is stored for the night. If the energy storage is neglected, the thermal efficiency becomes more than 30%. Second, the denominator is the sun beam energy which has reached the receiver surface. If the once collected energy on the receiver surface is used for the denominator, the thermal efficiency becomes 25%. Therefore, the above values of the thermal efficiency are not so low though the thermal efficiency values for the existing commercial plants provided with molten salt cooling and energy storage system are not published. Figures 12, 13 and 14 show the energy balances for the supercritical CO_2 cycle with 60.5mm tube, the supercritical CO_2 cycle with 46.8mm tube and the Brayton CO_2 cycle, respectively. These figures clarify the above issues.

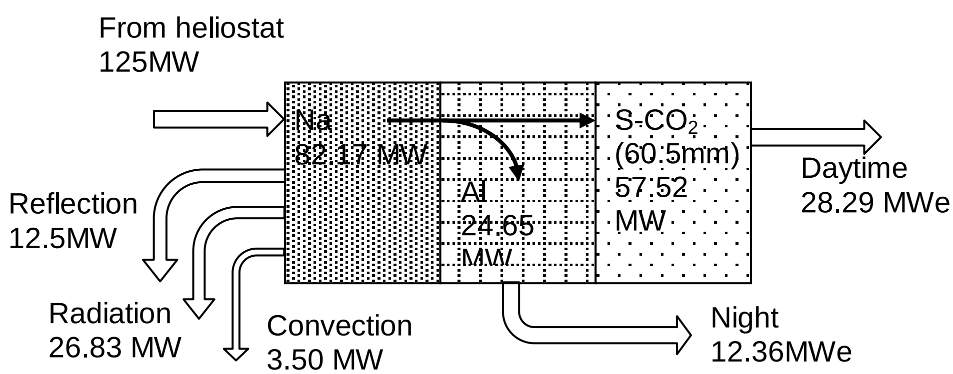

Fig. 10. Energy balance of the solar thermal power system with supercritical CO_2 GT with 60.5 mm diameter tube.

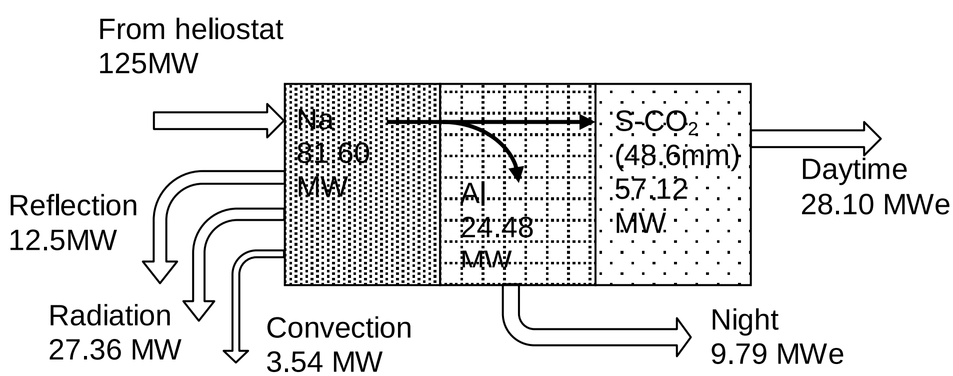

Fig. 10. Energy balance of the solar thermal power system with supercritical CO_2 GT with 48.6 mm diameter tube.

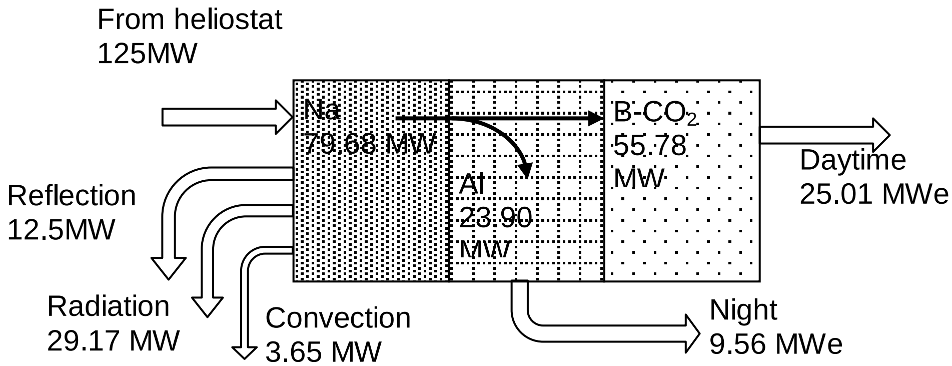

Fig. 11. Energy balance of the solar thermal power system with Brayton CO_2 GT.

In the final decision, capital costs and operation costs should be considered. In the solar thermal power plants, there is no fuel cost. Therefore, the higher thermal efficiency is only important in the meaning that it results in the lower capital cost. In the above cases, both the capital cost and the operation cost must be higher for the supercritical CO_2 cycle than for the Brayton CO_2 cycle. Therefore, it is not known whether the above 2.5% advantage in the thermal efficiency for the supercritical CO_2 cycle exceeds the demerit in both the capital cost and the operation cost or not. More comprehensive studies are needed.

RECUPERATOR DESIGN

Regarding both turbine designs and compressor designs, almost the same characteristics are obtainable. No great difference is expected between the supercritical CO_2 GT and the Brayton CO_2 GT, except that the compressor designs are somewhat difficult for the supercritical machines. The recuperator designs are described here. For cases achieving the maximum thermal efficiency of the total system, the design conditions are presented in Table 4.

Table 4. Design conditions of recuperator modules

Items		Supercritical CO_2 gas turbine		Brayton CO_2 GT
		RHX-1	RHX-2	RHX
Number of modules		6	6	6
Heat load MW/module		11.012	4.884	8.950
HT side	Flow rate kg/s	32.887	32.887	26.248
	Inlet temperature	503.25	209.70	430.84
	Inlet pressure MPa	6.410	6.333	1.305
LT side	Flow rate kg/s	32.887	19.598	26.248
	Inlet temperature °C	196.69	67.39	92.67
	Inlet pressure MPa	20.283	20.365	8.113

The PCHE with S-shape fins has been used as described in an earlier paper. Results of design calculations are presented in Table 5. There is no distinct difference between the recuperators for the supercritical CO_2 and the recuperator for the Brayton CO_2.

Table 5. Results of recuperator designs

Items		Supercritical CO_2 gas turbine		Brayton CO_2 GT
		RHX-1	RHX-2	RHX
Width × Length	m/ module	0.26 × 1.0	0.26 × 1.0	0.26 × 0.88
Height	m/ module	5.72	3.25	9.26
Weight	ton/ module	10.66	6.25	15.19
Total weight	ton	64.0	37.5	91.1
Heat transfer capacity	MW	11.023	4.892	8.967
Pressure loss ratio (dP/ Pinlet)	High T. side %	0.227	0.383	0.931
	Low T. side %	0.252	0.040	0.074

CONCLUSIONS

Values of the cycle thermal efficiency of two CO_2 GT cycles, i.e., 20 MPa supercritical CO_2 GT cycle and 8 MPa Brayton CO_2 GT cycle, applied to solar thermal power plants have been compared. The solar power plant consists of the following components: the tower-top solar collecting system; the sun-energy receiver cooled by Na; the Na-Al-CO_2 heat exchanger, which is also used for thermal energy storage; and the CO_2 gas turbine with 650°C turbine inlet temperature. The CO2 inlet temperatures are fixed to achieve the maximum cycle thermal efficiency. The 30% thermal energy is stored in the aluminum for the power generation in the night. Performance of the receiver, the heat exchanger and the CO_2 gas turbine cycles were explained in this report. The value of the receiver efficiency decreases with the Na inlet temperature. In the Na-Al-CO_2 heat exchanger design, the values of the horizontal tube spacing are varied and adjusted to the required heat load. As results of design calculations, the values of the receiver inlet temperature of 600°C, 610°C and 640°C were selected for the 20 MPa supercritical CO_2 with 60.5mm tube, for the 20 MPa supercritical CO_2 with 48.6mm tube and for the 8 MPa Brayton CO_2, respectively. The total thermal efficiency of the solar power generation system is around 2.5% higher for the supercritical CO_2 cycle than that for the Brayton CO_2 cycle. For the final decision, however, more comprehensive design studies must be done including estimations of both the capital cost and the operation cost.

NOMENCLATURE

BC = bypass compressor
GT = gas turbine
HPC = high-pressure compressor
IC = intercooler
LPC = low-pressure compressor
MPC = medium pressure compressor
PCHE = four-way printed circuit heat exchanger
PC = precooler
RHX = recuperative heat exchanger

REFERENCES

Hasuike, H., Yoshizawa, Y., Suzuki, A., Tamaura, Y., 2006, “Study on design of molten salt solar receivers for beam-down solar concentrator,” Solar Energy, 80, 1255-1262.

Kato, Y., Nitawaki, T., Muto, Y., 2004, "Medium temperature carbon dioxide gas turbine reactor," Nuclear Engineering and Design, 230, 195-207.

Muto, Y., Aritomi, M. Ishizuka, T., and Watanabe, N., 2014, "Comparison of supercritical CO_2 gas turbine cycle and Brayton CO_2 gas turbine cycle for solar thermal power plants," *Proc. of fourth International Symposium – Supercritical CO_2 Power Cycles*, Pittsburgh, USA, September 9–10, Paper 50.

Muto, Y., Ishizuka, T., and Aritomi, M., 2010, "Conceptual design of a commercial supercritical CO_2 gas turbine for the fast reactor power plant," *Proc. of ICAPP'10*, San Diego, USA, June 13–17, Paper 10102.

Muto, Y., Kato, Y., 2013, "Cycle Thermal Efficiency of Supercritical CO_2 Gas Turbine Dependent on Recuperator Performance," Journal of Power and Energy Systems, Vol.7, No. 3.

PROPATH group, 1990, "PROPATH: *A Program Package for Thermo-physical Properties of Fluids, Version 10.2*," Corona Publishing Co., Tokyo, Japan.